

LocalStyleFool: Regional Video Style Transfer Attack Using Segment Anything Model

Yuxin Cao[†], Jinghao Li[‡], Xi Xiao^{†*}, Derui Wang[§], Minhui Xue[§], Hao Ge[¶], Wei Liu^{||}, Guangwu Hu^{||*}

[†]*Shenzhen International Graduate School, Tsinghua University, China*

[‡]*Shandong University, China*

[§]*CSIRO's Data61, Australia*

[¶]*Ping An Technology, China*

^{||}*Shenzhen Institute of Information Technology, China*

Abstract—Previous work has shown that well-crafted adversarial perturbations can threaten the security of video recognition systems. Attackers can invade such models with a low query budget when the perturbations are semantic-invariant, such as StyleFool. Despite the query efficiency, the naturalness of the minutia areas still requires amelioration, since StyleFool leverages style transfer to all pixels in each frame. To close the gap, we propose LocalStyleFool, an improved black-box video adversarial attack that superimposes regional style-transfer-based perturbations on videos. Benefiting from the popularity and scalably usability of Segment Anything Model (SAM), we first extract different regions according to semantic information and then track them through the video stream to maintain the temporal consistency. Then, we add style-transfer-based perturbations to several regions selected based on the associative criterion of transfer-based gradient information and regional area. Perturbation fine adjustment is followed to make stylized videos adversarial. We demonstrate that LocalStyleFool can improve both intra-frame and inter-frame naturalness through a human-assessed survey, while maintaining competitive fooling rate and query efficiency. Successful experiments on the high-resolution dataset also showcase that scrupulous segmentation of SAM helps to improve the scalability of adversarial attacks under high-resolution data.

1. Introduction

With the tentacles of deep learning extending to various computer vision applications in daily life, *e.g.*, autonomous driving [1], smart home [2] and virtual/augmented reality [3], its success and convenience have benefited most ordinary people. However, everything is a double-edged sword: Deep Neural Networks (DNNs) are found to be vulnerable to adversarial examples generated by minuscule imperceptible perturbations that can mislead the classifier [4], [5]. This decade-long discovery has posed a threat to the security of DNNs in both academia and industry. Despite the popularity of short videos in today's era, video recognition models cannot escape by sheer luck from adversarial attacks. Therefore,

comprehensive research on video adversarial attacks is in great demand.

In the early stage, studies are centered on restricted adversarial attacks in which perturbations are constrained within the ℓ_p norm ball around the clean input [6], [7], [8], [9]. Such attacks keep the requirement of image attacks that perturbations are imperceptible both mathematically and visually. However, the negligible perturbations require large amounts of queries when the adversary has no access to the surrogate model (black-box setting). Recently, some scholars have proposed a new branch of attack: unrestricted attacks, where the adversary can enlarge the perturbation size to make the perturbations as imperceptible as possible. This kind of semantic-invariant attack can be roughly divided into patch-based attacks and style-based attacks. Despite the efficiency improvement and strong capability to bypass adversarial defenses, there are significant flaws in naturalness and temporal consistency. Patches such as bullet-screen comments [10], and semantically unrelated stickers [11], are obvious enough to alert people. StyleFool [12] is the first attempt to introduce style transfer to video attack. It elaborately designs a style selection strategy to change the style of all pixels in each frame, ensuring temporal consistency and overall naturalness. However, such practice inevitably brings about a local color abnormality that is counterfactual to human cognition, *i.e.*, green skin.

To bridge the gap mentioned above, we propose a novel black-box attack for video recognition models called LocalStyleFool. As an improvement of StyleFool, our attack considers adding style transfer in several regional areas using different but natural style images. Concretely, we first use the Segment Anything Model (SAM) [13] to extract different semantic regions, and then find several important regions which are at the top of an associative criterion of the Grad-CAM (Gradient-weighted Class Activation Mapping) [14], [15] output for a local pre-trained image model and the regional area. Afterwards, these regions are tracked through the video stream and transferred by different style images extracted from the target class video. Finally, similar to StyleFool, the perturbations are fine-adjusted to ensure misclassification. We conduct a user study to showcase the advantage of both intra-frame and inter-frame naturalness

* *Corresponding authors.*

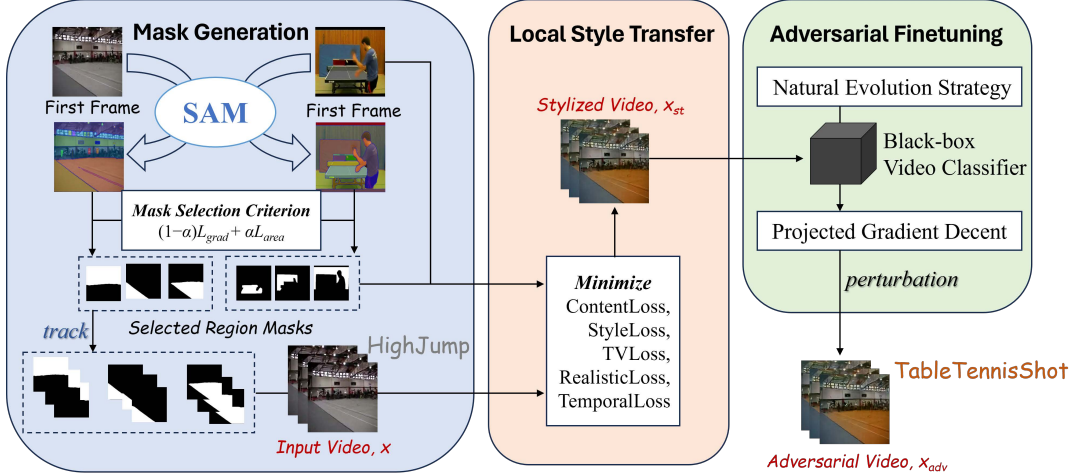


Figure 1. Overview of LocalStyleFool.

compared with StyleFool, while maintaining competitive attack efficiency. Experiments on a high-resolution video dataset, Kinetics-700 [16], also show that refined style-transfer-based perturbations in high-resolution videos can help improve video quality and avoid local counterfactual details. Despite the positive benefits of SAM, we manifest that it can also be used to malicious or illegal behavior, such as forging adversarial examples.

Our main contributions are summarized as follows.

- We improve StyleFool and propose LocalStyleFool, a new black-box video adversarial attack on video models, leveraging style transfer to different semantic regions using different style images. This closes the gap in the naturalness insufficiency of StyleFool.
- LocalStyleFool requires competitive query budgets but improves regional naturalness in the frame and temporal consistency across frames, which is verified by comprehensive experiments and a human-accessed survey.
- LocalStyleFool also witnesses excellent attack performance on the high-resolution video dataset, catering to the video development trend. To the best of our knowledge, we are the first to employ the Segment Anything Model to conduct malicious adversarial attacks. We hope to increase the attention of the security community to the negative impacts of such techniques.

1.1. Restricted Video Attacks

Early study focused on the white-box setting, where the structure and parameters of the model are available to the adversary [6], [8], [17]. The perturbations were required to ensure stealthiness under the ℓ_p norm restriction. Since the black-box setting has won better popularity and is more pragmatic, numerous black-box attacks have come into sight in academia these years [7], [9], [18], [19]. In addition, reinforcement learning has been widely used to optimize high-dimensional perturbations or extract key frames and regions to enhance sparsity [20], [21], [22], [23]. There

is also some work on cross-modal attacks that generated video perturbations from images/image models [24], [25]. However, redundant queries lead to low attack efficiency.

1.2. Unrestricted Video Attacks

To make the perturbations larger and reduce the query budget, some research considered unrestricted perturbations which are not related to video semantics. This branch of attacks includes changing style [12], [26] and adding patches [11], flickers [27], extra frames [28] or bullet-screen comments [10]. StyleFool [12] fools video classifiers by introducing natural style transfer to initialize the input video. However, the overall style transfer brings about color and texture distortion in local areas, which is not in line with human cognition and natural laws. In order to make perturbations more natural, Chen et al. [10] added large bullet-screen comments to the video, but this attack is not suitable for targeted attacks, which was later verified by Jiang et al. [11] They added patch-based perturbations to the video, but the patches are not semantically related to the original input video, and the perturbation range is so large that human perception systems can easily be aware of the perturbations. Also, some large patches directly obscure the core action area of the video. Overall, most unrestricted perturbations were much too obvious in the level of both intra-frame (*e.g.*, weird patches, counterfactual details) and inter-frame (*e.g.*, erratic transitional flicker), bringing about lack of naturalness and temporal inconsistency.

2. Method

2.1. Preliminary

We assume a DNN video recognition model f which takes a video x with T frames as input. The output of the model f includes the predicted label y and its confidence score. We assume that the adversary launches the attack

under a query-limited black-box setting where only the top-1 label and its score are accessible, and there is a query limit for the attack, since the higher query budget lacks practicality in real-world scenarios. Moreover, the adversary can choose the attack goal from targeted attacks and untargeted attacks. The adversarial video x_{adv} should be misclassified to a predefined target class y_t in targeted attacks, *i.e.*, $f(x_{adv}) = y_t$, while to any class other than the ground-truth class y_0 in untargeted attacks, *i.e.*, $f(x_{adv}) \neq y_0$. We provide the overview of LocalStyleFool in Figure 1.

2.2. Mask Generation

Adversarial videos generated by StyleFool (as shown in Figure 2) are found unnatural in regional details, since StyleFool applies style transfer to all pixels of each frame. To improve this gap, an intuitive alternative is to introduce different style transfer to different regions. However, a pilot study conducted ourselves shows that it is rather difficult to segment different semantic regions in the resized videos. This conclusion is based on two fundamental facts. 1) Existing video attacks design and optimize perturbations after resizing the video to the input size requirement of the surrogate model. It is of nature and reality, since the video that is projected to misclassify the model is the resized video. 2) Most existing widely used video recognition models (*e.g.*, C3D [29], I3D [30]) require the input videos to be resized to a low resolution (lower than 224×224), making it difficult to apply object segmentation methods. These facts prompt us to consider designing perturbations on the original high-resolution videos. Thanks to the SAM [13] proposed recently, it is a relatively convenient alternative to introduce SAM to video adversarial attacks.

Due to the advantages of zero-hot transferability and accurate segmentation in high-resolution images, SAM has been used in various fields [31]. In our task, we first use pre-trained SAM to extract the masks for the first frame of the video. According to some existing work focusing on adding sparse perturbations to videos [21], [22], different regions make different contributions to the prediction of the recognition model. Therefore, we choose some of the regions from the output masks of SAM to perform style transfer. To be specific, we design an associative criterion to choose the regions to be style-transferred.

Transfer-based gradient information. In black-box attacks, the adversary has no access to the model architecture. Due to the transferability of adversarial perturbations across models [32] and data domains (from images to videos) [7], [24], we utilize a local white-box image model to obtain the significance of different regions by Grad-CAM [14]. Concretely, we first use a pre-trained ResNet-50 [33] model g to obtain the heatmap for class y_c :

$$H^{y_c} = \text{ReLU} \left(\frac{1}{SR} \sum_k \sum_{i,j} \frac{\partial g(y_c|x_1)}{\partial F_{i,j}^k} F^k(x_1) \right), \quad (1)$$

where ReLU represents the ReLU activation function, F^k represents the k -th feature map for the first frame x_1 , (i, j) denotes the pixel position of the image, SR denotes the

spatial resolution of the feature map. We use the first frame since one-action short video has no manifest difference across frames [12].

We use M^p to represent the mask matrix for the p -th region of the output of SAM, which is a sparse matrix, in which the pixel belonging to this segmentation region is set to 1, otherwise 0. Assuming that SAM outputs N regions m_1, m_2, \dots, m_N ($m_i \cap m_j = \emptyset, \forall i, j \in \{1, 2, \dots, N\}, i \neq j$) and their corresponding masks M^1, M^2, \dots, M^N , the normalized gradient significance can be expressed as

$$L_{grad}(p) = \frac{\sum_{(i,j) \in m_p} M_{i,j}^p H_{i,j}^{y_c} - \min_q \sum_{(i,j) \in m_q} M_{i,j}^q H_{i,j}^{y_c}}{\max_q \sum_{(i,j) \in m_q} M_{i,j}^q H_{i,j}^{y_c} - \min_q \sum_{(i,j) \in m_q} M_{i,j}^q H_{i,j}^{y_c}}, \quad (2)$$

where m_p denotes the p -th region.

Regional area. There is no direct relationship between the gradient significance and the regional area. In some cases, the areas of the top-ranked segmentation regions are very small, increasing the attack difficulty. That is to say, the cost-effectiveness of style transfer in these small regions is very low: complex calculations are required, but the impact on the classifier is minimal. To prioritize style transfer from regions with larger areas, we additionally consider the regional area as another criterion for choosing segmentation regions. Then, we consider the normalized area significance:

$$L_{area}(p) = \frac{\|M^p\|_0 - \min_q \|M^q\|_0}{\max_q \|M^q\|_0 - \min_q \|M^q\|_0}. \quad (3)$$

Associative criterion. Since the gradient information and regional area contribute differently to the attack, we use the weighted significance criterion as follows.

$$L_{total}(p) = (1 - \alpha) L_{grad}(p) + \alpha L_{area}(p), \quad (4)$$

where α denotes the weight coefficient. Then we obtain the masks $\mathcal{M}^1, \mathcal{M}^2, \dots, \mathcal{M}^N$ by sorting them in descending order according to L_{total} . However, the total area of the top-ranked regions is still different among videos. Therefore, to ensure that all adversarial videos have similar perturbed areas, we further set a total area lower bound. Concretely, we select the top- r regions which satisfies that

$$r = \arg \max_{r'} r', \text{ s.t. } \sum_{p=1}^{r'-1} \|\mathcal{M}^p\|_0 \leq \mu \sum_{p=1}^N \|\mathcal{M}^p\|_0 \quad (5)$$

where μ represents the total area lower bound coefficient.

2.3. Style Transfer

Stylized videos will become unnatural and contrary to human cognition if the style images are selected randomly. Save for the visual naturalness brought by color, StyleFool uses target class confidence to move stylized videos close to the decision boundary, which shows that style images from the target class carry a lot of target class information. Therefore, we select the target class video with the highest confidence score in the targeted class, while a random video from the class other than the original class in untargeted attacks. To make stylized videos more natural, we consider the image with different style regions. We first use the

associative criterion in Equation 4 to obtain the top- r masks $\Psi^1, \Psi^2, \dots, \Psi^r$ for target class video x_t . Then, the r regions of the original video x will undergo style transfer using the style images s as the r regions of the target class video x_t . In content loss and style loss, we use VGG-19 [34] to obtain high-level features. We improve the style loss to:

$$L_{\text{style}}(x^s, s) = \sum_l \sum_p \frac{1}{C_l^2} \|G_{l,p}(s) - G_{l,p}(x^s)\|_2^2, \quad (6)$$

where s denotes the style image from the target class video, x^s denotes the stylized video frame, C_l denotes the channel number in the l -th layer, $G_{l,p}$ denotes the Gram matrix [35] corresponding to the feature $Q_{l,p}$ of the VGG-19 model. For s and x^s , the features are expressed as

$$\begin{aligned} Q_{l,p}(s) &= \Psi_l^p Q_l(s) \\ Q_{l,p}(x^s) &= \mathcal{M}_l^p Q_l(x^s), \end{aligned} \quad (7)$$

where the subscript l represents the l -th layer. The masks are downsampled to match the feature map in the l -th layer.

We additionally consider total variance loss and realistic loss [36] to improve the smoothness at the spatial level. The realistic loss is built based on Matting Laplacian [37], which can penalize unnatural distortion to produce stylized photorealistic video frames. Similar to StyleFool [12], we introduce temporal loss to maintain the temporal consistency and leverage the Natural Evolution Strategy (NES) [38] and Projected Gradient Decent (PGD) [39] to finetune the perturbations after video style transfer. Note that the masks change through the video stream. We use the Track Anything Model (TAM) [40] to track the top- r regions with masks $\mathcal{M}^1, \mathcal{M}^2, \dots, \mathcal{M}^r$ in the original video to maintain temporal consistency. The r styles extracted from the target class video remain unchanged. Algorithm 1 briefly describes the procedure of LocalStyleFool.

3. Experiments

3.1. Experimental Setup

Datasets. Similar to most work on video adversarial attack tasks [10], [12], [17], [22], [41], we select UCF-101 [42] and HMDB-51 [43] as our datasets due to their popularity and comprehensiveness. UCF-101 [42] consists of 13,320 videos from 101 classes. HMDB-51 [43] contains 6,849 videos from 51 classes. We also include Kinetics-700 [16], which contains approximately 650,000 videos from 700 classes. The resolution of the videos in Kinetics-700 is higher than that of UCF-101 and HMDB-51, with more than 40% videos having a resolution of 1280×720 or higher. All videos were compiled from YouTube and contained only one action.

Models. We choose C3D [44] and I3D [30] as surrogate models for UCF-101 and HMDB-51 because they are used most frequently for video recognition tasks. C3D learns temporal features by 3D convolution, while I3D uses optical flow to obtain transitional information between consecutive frames. We train the models ourselves before the attack. For Kinetics-700, we replace C3D with R3D [45] due to better

Algorithm 1: LocalStyleFool.

Input: Black-box model f , input video x , target class y_t , significance criterion L_{total} , style transfer loss L_{st} .
Output: Adversarial video x_{adv} .

- 1 $x_{(1)} \leftarrow$ the first frame of x ;
- 2 $x_t \leftarrow$ target class video;
- 3 $s \leftarrow$ the first frame of x_t ;
- 4 $M^1, M^2, \dots, M^N \leftarrow \text{SAM}(x_{(1)})$;
- 5 $\psi^1, \psi^2, \dots, \psi^N \leftarrow \text{SAM}(s)$;
- 6 $\mathcal{M}_{(1)}^1, \mathcal{M}_{(1)}^2, \dots, \mathcal{M}_{(1)}^r \leftarrow$ top- r masks sorted by L_{total} ;
- 7 $\mathcal{M}_{(2)}^{1,2,\dots,r}, \dots, \mathcal{M}_{(T)}^{1,2,\dots,r} \leftarrow \text{TAM}(x, \mathcal{M}_{(1)}^{1,2,\dots,r})$;
- 8 $\mathcal{M} \leftarrow \{\mathcal{M}_{(1)}^{1,2,\dots,r}, \mathcal{M}_{(2)}^{1,2,\dots,r}, \dots, \mathcal{M}_{(T)}^{1,2,\dots,r}\}$;
- 9 $\Psi^1, \Psi^2, \dots, \Psi^r \leftarrow$ top- r masks sorted by L_{total} ;
- 10 $\Psi \leftarrow \{\Psi^1, \Psi^2, \dots, \Psi^r\}$;
- 11 $x_{st} \leftarrow \text{ST}(\mathcal{M}, \Psi, x, s, L_{st})$;
- 12 $x_{adv} \leftarrow \text{Finetune}(x_{st}, y_t, x_t, f)$.

recognition performance of 3D ResNet models. We use the pre-trained model provided for Kinetics-700 [46]. The test dataset accuracy for UCF-101 is 85.2% (C3D) and 86.9% (I3D), for HMDB-51 is 67.0% (C3D) and 62.8% (I3D), and for Kinetics-700 is 68.4% (I3D) and 63.1% (R3D).

Metrics. Following StyleFool [12], we use Attack Success Rate (ASR) and Minimal Queries (minQ), Maximal Queries (maxQ), and Average Queries (AQ) as our main metrics to evaluate quantitative attack performance. ASR stands for the ratio of successful attacks where the video is misclassified. The metrics related to queries showcase the attack efficiency. Note that the attack performance is also largely influenced by imperceptibility, which can be determined by visual perception by human subjects.

Competitors. Since there are not many unrestricted attacks for videos, we choose two which are close to ours, STDE [11], StyleFool [12]. STDE superimposes part of the regions in other videos on the input video, which achieves fewer queries, but the naturalness of adversarial videos is largely sacrificed. The patch is abrupt, large in size, lacks relevance to the semantics of the original video, and may obscure the important content of the original video. Although StyleFool achieves high attack efficiency while maintaining overall imperceptibility, local counterfactual colors and unnatural details still exist if videos are watched carefully. Please refer to the appendix for more experimental details and discussion on comparison with other video attacks.

Fairness. Due to different techniques and experimental setups in STDE and StyleFool, it is not scalable and meaningful to modify them to the same framework as LocalStyleFool, e.g., aligning to the same ℓ_p norm. Enlarging the ℓ_p norm for STDE will lead to fewer queries but to a more obvious patch, while the ℓ_p norm for StyleFool varies according to different style images. As a result, we use the default parameters for STDE and StyleFool, and focus more on the imperceptibility of visualization.

3.2. Results and Analyses

We randomly select 150 videos from all datasets and conduct LocalStyleFool as well as the other two competi-

TABLE 1. ATTACK PERFORMANCE COMPARISON ON UCF-101.

Model	Attack	UCF-101 (Targeted)				UCF-101 (Untargeted)			
		ASR	minQ	maxQ	AQ	ASR	minQ	maxQ	AQ
C3D	STDE [11]	100	91	5,684	2,910	100	16	4,320	2,820
	StyleFool [12]	100	1,322	273,446	73,104	100	1	18,772	3,676
	LocalStyleFool	100	1,274	215,932	70,425	100	1	19,072	3,575
I3D	STDE [11]	100	30	4,638	1,653	100	30	3,688	1,532
	StyleFool [12]	100	101	122,740	32,074	100	1	29,517	6,557
	LocalStyleFool	100	101	117,481	33,472	100	1	31,409	7,052

TABLE 2. ATTACK PERFORMANCE COMPARISON ON HMDB-51.

Model	Attack	HMDB-51 (Targeted)				HMDB-51 (Untargeted)			
		ASR	minQ	maxQ	AQ	ASR	minQ	maxQ	AQ
C3D	STDE [11]	100	30	5,598	2,165	100	16	3,754	1,849
	StyleFool [12]	100	101	98,715	38,804	100	1	10,998	2,032
	LocalStyleFool	100	101	104,355	41,833	100	1	18,474	2,438
I3D	STDE [11]	100	30	4,896	1,623	100	19	6,879	1,835
	StyleFool [12]	100	101	79,418	24,078	100	1	6,510	2,290
	LocalStyleFool	100	101	95,330	23,174	100	1	8,372	1,614

tors. Tables 1, 2 and 3 report the quantitative results. Note that the queries during the target class video selection are counted. Figure 2 shows the visualization. Since STDE adds large, unrestricted patches to the clean videos, the attack is the most query-efficient. However, the patches are so obtrusive that they even occlude the semantic region of the original action in the clean video. Even if STDE can quickly fool the video recognition model, this significant flaw in naturalness can directly lead to the failure of the attack: relevant personnel can easily perceive anomalies and trigger alarms. Compared to STDE, StyleFool requires more queries, but improves imperceptibility by a large margin. StyleFool transfers the clean video to another style for all pixels and, through an accurate and rigorous style selection strategy, achieves good naturalness. However, the overall style transfer can lead to unnatural regional details, *e.g.*, the green face and skin in Figure 2. As an improvement, LocalStyleFool closes this gap and further enhances the naturalness by conducting style transfer on different regions, while maintaining comparable query cost. We provide examples of LocalStyleFool when conducting style transfer on one region in Figure 2 and multiple regions in Figure 3 (last row). Results on Kinetics-700 indicate that performing style transfer on the high-resolution video first and then inputting it into the victim model is beneficial for improving attack efficiency.

We also record the one-query attack success rate (1Q-ASR) to demonstrate the effectiveness of our method. The 1Q-ASR refers to the rate of clean videos that are immediately classified into target class (in targeted attacks) or any other class (in untargeted attacks) after style transfer. Thus, there is no need for the subsequent perturbation optimization. On average, LocalStyleFool achieves a 1Q-ASR of over 8% in targeted attacks and 53% in untargeted attacks. Especially, the 1Q-ASR achieves 81.3% when attacking R3D on Kinetics-700 in the untargeted setting, which means that video recognition systems are extremely vulnerable to non-semantic perturbations which can push the stylized videos across the decision boundary at ease. We provide the discussion on potential mitigation in the appendix.

TABLE 3. ATTACK PERFORMANCE COMPARISON ON KINETICS-700.

Model	Attack	Kinetics-700 (Targeted)				Kinetics-700 (Untargeted)			
		ASR	minQ	maxQ	AQ	ASR	minQ	maxQ	AQ
R3D	STDE [11]	100	182	32,065	8,731	100	16	5,654	1,810
	StyleFool [12]	100	101	78,455	19,204	100	1	8,538	724
	LocalStyleFool	100	101	80,335	17,098	100	1	7,265	598
I3D	STDE [11]	100	107	48,962	15,651	100	30	6,547	3,205
	StyleFool [12]	100	101	122,481	24,573	100	1	12,601	1,536
	LocalStyleFool	100	101	113,472	25,307	100	1	9,914	1,298

3.3. User Study

Apart from quantitative analyses, we also conduct a human-centered census to show the indistinguishability of the proposed LocalStyleFool, which is a supplement to the visualization effect from a human perspective. We conducted an online survey on Amazon Mechanical Turk [47] and recruited 100 anonymous subjects over 18 years of age. All subjects are from English-speaking countries and can complete the survey in English. Following most user studies in similar adversarial attack tasks [12], [48], our survey consists of three parts, naturalness, realness, and consistency. Subjects were paid \$0.8 for each question.

Naturalness: The naturalness refers to the degree to which its color, texture, and overall appearance are consistent with human basic cognition. We randomly selected 20 clean videos and their corresponding adversarial counterparts for three attacks. The subjects were asked to evaluate the naturalness based on a Likert-scale [49] from 1 to 5. A higher score indicates more natural.

Realness: The realness refers to the degree to which it appears to be shot realistically in the real world, with almost no traces of artificial processing. We then grouped the videos to ask the subjects to distinguish the realness.

Consistency: The consistency includes spatial consistency (smoothness of value changes between a pixel and its surrounding pixels) and temporal consistency (smoothness and coherence of transitions between frames). We randomly selected another 40 videos, 10 from each attack, and asked the subjects to rate the consistency from 1 to 5. A higher score indicates greater consistency. The order of the videos was randomly shuffled to avoid potential bias.

Analyses. We finally obtained 97 valid questionnaires after filtering out 3 questionnaires whose complete time is much shorter than the total time for playing all videos. Table 4 reports the average naturalness and consistency results obtained from subjects. Although STDE requires the least queries by adding large patches to the video, naturalness is greatly sacrificed, which can easily trigger alerts and finally lead to a futile attack. Patches are conspicuous and inserted into sparse frames, which also greatly reduces the consistency rate. StyleFool improves naturalness and consistency greatly since it considers fine style selection to ensure the stylized video not only maintains good imperceptibility but is also close to the decision boundary. However, style transferring on all pixels leads to counter-cognitive details in local areas such as aberrant colors and texture. LocalStyleFool closes this gap and obtains higher naturalness and consistency rates that are closest to those of clean videos.



Figure 2. Visualization of different video attacks.

TABLE 4. RESULTS OF NATURALNESS AND CONSISTENCY TESTS.

	STDE	StyleFool	LocalStyleFool	Clean
Naturalness	2.32	3.06	3.45	3.60
Consistency	1.91	3.24	3.65	3.92

TABLE 5. RESULTS OF REALNESS TEST.

	LocalStyleFool is real	Another one is real	Both real	Both unreal
LocalStyleFool-STDE	51.5%	6.2%	10.3%	32.0%
LocalStyleFool-StyleFool	40.2%	20.6%	29.9%	9.3%
LocalStyleFool-Clean	34.0%	37.1%	26.8%	2.1%

Table 5 reports the realness test results. Compared to STDE, 51.5% of the subjects thought LocalStyleFool is real while this figure was only 6.2% for STDE. As analyzed previously, the unnatural patch of STDE reduces video quality and makes people feel that the videos have been maliciously modified. Over 40% of the subjects consented that LocalStyleFool generated more real videos than StyleFool, showing the outstanding advantage of LocalStyleFool in maintaining local smooth details. Nearly 30% of the subjects considered both videos were real, indicating that the style-transfer-based perturbations carry high stealthiness. It is surprising that up to 34.0% of the subjects rooted for LocalStyleFool, while clean videos only obtained 37.1% of the votes. This shows that LocalStyleFool can achieve high verisimilitude similar to clean videos.

3.4. Ablation Study

LocalStyleFool considers transfer-based gradient information and regional area at the region selection stage. To explore the contribution of these two criteria to the attack, we conduct an ablation study. As a control, we randomly select regions in the original video before conducting style transfer. Then, we ablate the gradient information ($\alpha = 1$) and regional area restriction ($\alpha = 0$) respectively. We randomly select 50 videos from UCF-101 and attack the C3D model. Figure 3 shows the visualization of an example. When the region is randomly selected or only based on the gradient information, the color and texture tend to be

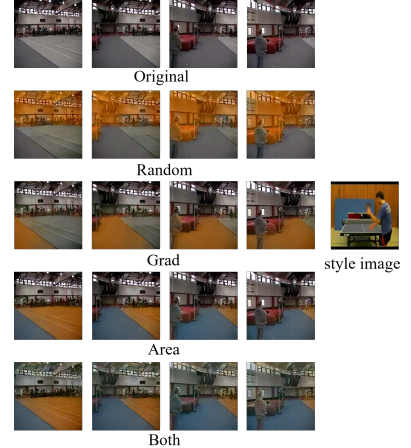


Figure 3. Visualization of ablation study.

unnatural, which can cause alarm. Also, the attack becomes difficult or even vain if the regions selected based on gradient information are rather small. When only the regional area is considered, the selected areas may not overlap with the dominant regions of the original video, which requires an additional average of over 12% queries. Overall, only when both two criteria are considered can LocalStyleFool achieve both high attack efficiency and sensory comfort, *e.g.*, the playing field seems to have only been renovated as shown in the last row.

4. Conclusion

To address the problem of low naturalness in local areas in the existing style-transfer-based attack, we propose LocalStyleFool, which adds regional style-transfer-based perturbations to ameliorate the video quality based on SAM. We design an associative criterion of the combination of transfer-based gradient information and regional area to select the regions for style transfer and track these regions through the video stream. According to the user study, the adversarial videos generated by LocalStyleFool improve the imperceptibility in terms of naturalness, realness, and consistency while maintaining competent attack efficiency. SAM also helps LocalStyleFool to consume fewer queries in high-resolution data and avoid regional artifacts. Our work also exposes the negative aspect of SAM if misused for malicious purposes. We will plumb possible defenses for style-transfer-based attacks in the future.

5. Acknowledgments

This work was supported in part by the Overseas Research Cooperation Fund of Tsinghua Shenzhen International Graduate School (HW2021013), Guangdong Basic and Applied Basic Research Foundation (2022A1515010417) and the Key Project of Shenzhen Municipality (JSGG20211029095545002).

References

- [1] Ekim Yurtsever, Jacob Lambert, Alexander Carballo, and Kazuya Takeda. A survey of autonomous driving: Common practices and emerging technologies. *IEEE access*, 8:58443–58469, 2020.
- [2] Valentina Bianchi, Marco Bassoli, Gianfranco Lombardo, Paolo Fornacciaro, Monica Mordonini, and Ilaria De Munari. Iot wearable sensor and deep learning: An integrated approach for personalized human activity recognition in a smart home environment. *IEEE Internet of Things Journal*, 6(5):8553–8562, 2019.
- [3] Minglu Zhu, Zhongda Sun, Zixuan Zhang, Qiongfeng Shi, Tianyi He, Huicong Liu, Tao Chen, and Chengkuo Lee. Haptic-feedback smart glove as a creative human-machine interface (hmi) for virtual/augmented reality applications. *Science Advances*, 6(19):eaaz8693, 2020.
- [4] Christian Szegedy, Wojciech Zaremba, Ilya Sutskever, Joan Bruna, Dumitru Erhan, Ian Goodfellow, and Rob Fergus. Intriguing properties of neural networks. In *Proceedings of the International Conference on Learning Representations*, 2014.
- [5] Ian J Goodfellow, Jonathon Shlens, and Christian Szegedy. Explaining and harnessing adversarial examples. In *Proceedings of the International Conference on Learning Representations*, 2015.
- [6] Xingxing Wei, Jun Zhu, Sha Yuan, and Hang Su. Sparse adversarial perturbations for videos. In *Proceedings of the AAAI Conference on Artificial Intelligence (AAAI)*, volume 33, pages 8973–8980, 2019.
- [7] Linxi Jiang, Xingjun Ma, Shaoxiang Chen, James Bailey, and Yu-Gang Jiang. Black-box adversarial attacks on video recognition models. In *Proceedings of the 27th ACM International Conference on Multimedia*, pages 864–872, 2019.
- [8] Shasha Li, Ajaya Neupane, Sujoy Paul, Chengyu Song, Srikanth V Krishnamurthy, Amit K Roy-Chowdhury, and Ananthram Swami. Stealthy adversarial perturbations against real-time video classification systems. In *Proceedings of the Symposium on Network and Distributed Systems Security (NDSS)*, 2019.
- [9] Shasha Li, Abhishek Aich, Shitong Zhu, M. Salman Asif, Song Chengyu, Amit K. Roy-Chowdhury, and Srikanth Krishnamurthy. Adversarial attacks on black box video classifiers: Leveraging the power of geometric transformations. In *Advances in Neural Information Processing Systems*, volume 34, pages 2085–2096, 2021.
- [10] Kai Chen, Zhipeng Wei, Jingjing Chen, Zuxuan Wu, and Yu-Gang Jiang. Attacking video recognition models with bullet-screen comments. In *Proceedings of the AAAI Conference on Artificial Intelligence*, volume 36, pages 312–320, 2022.
- [11] Kaixun Jiang, Zhaoyu Chen, Hao Huang, Jiafeng Wang, Dingkan Yang, Bo Li, Yan Wang, and Wenqiang Zhang. Efficient decision-based black-box patch attacks on video recognition. In *Proceedings of the IEEE/CVF International Conference on Computer Vision*, pages 4379–4389, 2023.
- [12] Yuxin Cao, Xi Xiao, Ruoxi Sun, Derui Wang, Minhui Xue, and Sheng Wen. Stylefool: Fooling video classification systems via style transfer. In *2023 IEEE Symposium on Security and Privacy (SP)*, pages 1631–1648. IEEE, 2023.
- [13] Alexander Kirillov, Eric Mintun, Nikhila Ravi, Hanzi Mao, Chloe Rolland, Laura Gustafson, Tete Xiao, Spencer Whitehead, Alexander C Berg, Wan-Yen Lo, et al. Segment anything. *arXiv preprint arXiv:2304.02643*, 2023.
- [14] Ramprasaath R Selvaraju, Michael Cogswell, Abhishek Das, Ramakrishna Vedantam, Devi Parikh, and Dhruv Batra. Grad-cam: Visual explanations from deep networks via gradient-based localization. In *Proceedings of the IEEE international conference on computer vision*, pages 618–626, 2017.
- [15] Pytorch library for grad-cam. <https://github.com/jacobgil/pytorch-grad-cam>.
- [16] Joao Carreira, Eric Noland, Chloe Hillier, and Andrew Zisserman. A short note on the kinetics-700 human action dataset. *arXiv preprint arXiv:1907.06987*, 2019.
- [17] Guoming Wu, Yangfan Xu, Jun Li, Zhiping Shi, and Xianglong Liu. Imperceptible adversarial attack with multi-granular spatio-temporal attention for video action recognition. *IEEE Internet of Things Journal*, 2023.
- [18] Zhipeng Wei, Jingjing Chen, Xingxing Wei, Linxi Jiang, Tat-Seng Chua, Fengfeng Zhou, and Yu-Gang Jiang. Heuristic black-box adversarial attacks on video recognition models. In *Proceedings of the AAAI Conference on Artificial Intelligence (AAAI)*, volume 34, pages 12338–12345, 2020.
- [19] Zhipeng Wei, Jingjing Chen, Hao Zhang, Linxi Jiang, and Yu-Gang Jiang. Adaptive temporal grouping for black-box adversarial attacks on videos. In *Proceedings of the 2022 International Conference on Multimedia Retrieval*, pages 587–593, 2022.
- [20] Zeyuan Wang, Chaofeng Sha, and Su Yang. Reinforcement learning based sparse black-box adversarial attack on video recognition models. In *Proceedings of International Joint Conference on Artificial Intelligence*, 2021.
- [21] Huanqian Yan and Xingxing Wei. Efficient sparse attacks on videos using reinforcement learning. In *Proceedings of the 29th ACM International Conference on Multimedia*, pages 2326–2334, 2021.
- [22] Xingxing Wei, Huanqian Yan, and Bo Li. Sparse black-box video attack with reinforcement learning. *International Journal of Computer Vision*, 130(6):1459–1473, 2022.
- [23] Xingxing Wei, Songping Wang, and Huanqian Yan. Efficient robustness assessment via adversarial spatial-temporal focus on videos. *IEEE Transactions on Pattern Analysis and Machine Intelligence*, 2023.
- [24] Hee-Seon Kim, Minji Son, Minbeom Kim, Myung-Joon Kwon, and Changick Kim. Breaking temporal consistency: Generating video universal adversarial perturbations using image models. In *Proceedings of the IEEE/CVF International Conference on Computer Vision*, pages 4325–4334, 2023.
- [25] Ruikui Wang, Yuanfang Guo, and Yunhong Wang. Global-local characteristic excited cross-modal attacks from images to videos. In *Proceedings of the AAAI Conference on Artificial Intelligence*, volume 37, pages 2635–2643, 2023.
- [26] Yuxin Cao, Ziyu Zhao, Xi Xiao, Derui Wang, Minhui Xue, and Jin Lu. Logostylefool: Vitiating video recognition systems via logo style transfer. In *38th AAAI Conference on Artificial Intelligence*. AAAI, 2024.
- [27] Roi Pony, Itay Naeh, and Shie Mannor. Over-the-air adversarial flickering attacks against video recognition networks. In *Proceedings of the IEEE/CVF Conference on Computer Vision and Pattern Recognition*, 2021.
- [28] Zhikai Chen, Lingxi Xie, Shanmin Pang, Yong He, and Qi Tian. Appending adversarial frames for universal video attack. In *Proceedings of the IEEE/CVF Winter Conference on Applications of Computer Vision*, pages 3199–3208, 2021.
- [29] Shuiwang Ji, Wei Xu, Ming Yang, and Kai Yu. 3d convolutional neural networks for human action recognition. *IEEE transactions on pattern analysis and machine intelligence*, 35(1):221–231, 2012.
- [30] Joao Carreira and Andrew Zisserman. Quo vadis, action recognition? a new model and the kinetics dataset. In *proceedings of the IEEE Conference on Computer Vision and Pattern Recognition*, pages 6299–6308, 2017.
- [31] Maciej A Mazurowski, Haoyu Dong, Hanxue Gu, Jichen Yang, Nicholas Konz, and Yixin Zhang. Segment anything model for medical image analysis: an experimental study. *Medical Image Analysis*, 89:102918, 2023.
- [32] Nicolas Papernot, Patrick McDaniel, and Ian Goodfellow. Transferability in machine learning: from phenomena to black-box attacks using adversarial samples. *arXiv preprint arXiv:1605.07277*, 2016.

- [33] Kaiming He, Xiangyu Zhang, Shaoqing Ren, and Jian Sun. Deep residual learning for image recognition. In *Proceedings of the IEEE conference on computer vision and pattern recognition*, pages 770–778, 2016.
- [34] Karen Simonyan and Andrew Zisserman. Very deep convolutional networks for large-scale image recognition. *Proceedings of the International Conference on Learning Representations*, 2015.
- [35] Johnson Justin, Alahi Alexandre, and Feifei Li. Perceptual losses for real-time style transfer and super-resolution. In *Proceedings of the European Conference on Computer Vision (ECCV)*, 2016.
- [36] Fujun Luan, Sylvain Paris, Eli Shechtman, and Kavita Bala. Deep photo style transfer. In *Proceedings of the IEEE conference on computer vision and pattern recognition*, pages 4990–4998, 2017.
- [37] Anat Levin, Dani Lischinski, and Yair Weiss. A closed-form solution to natural image matting. *IEEE transactions on pattern analysis and machine intelligence*, 30(2):228–242, 2007.
- [38] Andrew Ilyas, Logan Engstrom, Anish Athalye, and Jessy Lin. Black-box adversarial attacks with limited queries and information. In *Proceedings of the 35th International Conference on Machine Learning*, pages 2137–2146. PMLR, 2018.
- [39] Aleksander Madry, Aleksandar Makelov, Ludwig Schmidt, Dimitris Tsipras, and Adrian Vladu. Towards deep learning models resistant to adversarial attacks. In *Proceedings of the International Conference on Learning Representations*, 2018.
- [40] Jinyu Yang, Mingqi Gao, Zhe Li, Shang Gao, Fangjing Wang, and Feng Zheng. Track anything: Segment anything meets videos. *arXiv preprint arXiv:2304.11968*, 2023.
- [41] Yixiao Xu, Xiaolei Liu, Mingyong Yin, Teng Hu, and Kangyi Ding. Sparse adversarial attack for video via gradient-based keyframe selection. In *ICASSP 2022-2022 IEEE International Conference on Acoustics, Speech and Signal Processing (ICASSP)*, pages 2874–2878. IEEE, 2022.
- [42] Khurram Soomro, Amir Roshan Zamir, and Mubarak Shah. Ucf101: A dataset of 101 human actions classes from videos in the wild. *arXiv preprint arXiv:1212.0402*, 2012.
- [43] Hildegard Kuehne, Hueihan Jhuang, Estíbaliz Garrote, Tomaso Poggio, and Thomas Serre. Hmdb: a large video database for human motion recognition. In *Proceedings of the IEEE/CVF International Conference on Computer Vision (ICCV)*, pages 2556–2563. IEEE, 2011.
- [44] Du Tran, Lubomir Bourdev, Rob Fergus, Lorenzo Torresani, and Manohar Paluri. Learning spatiotemporal features with 3d convolutional networks. In *Proceedings of the IEEE/CVF International Conference on Computer Vision (ICCV)*, pages 4489–4497, 2015.
- [45] Kensho Hara, Hirokatsu Kataoka, and Yutaka Satoh. Can spatiotemporal 3d cnns retrace the history of 2d cnns and imagenet? In *Proceedings of the IEEE conference on Computer Vision and Pattern Recognition*, pages 6546–6555, 2018.
- [46] 3d resnets for action recognition. <https://github.com/kenshohara/3D-ResNets-PyTorch/>.
- [47] Amazon mechanical turk. <https://www.mturk.com>.
- [48] Yunfeng Diao, Tianjia Shao, Yong-Liang Yang, Kun Zhou, and He Wang. Basar: black-box attack on skeletal action recognition. In *Proceedings of the IEEE/CVF Conference on Computer Vision and Pattern Recognition*, pages 7597–7607, 2021.
- [49] Rensis Likert. A technique for the measurement of attitudes. *Archives of psychology*, 1932.
- [50] Deqing Sun, Xiaodong Yang, Ming-Yu Liu, and Jan Kautz. Pwc-net: Cnns for optical flow using pyramid, warping, and cost volume. In *Proceedings of the IEEE conference on computer vision and pattern recognition*, pages 8934–8943, 2018.
- [51] Shangyu Xie, Han Wang, Yu Kong, and Yuan Hong. Universal 3-dimensional perturbations for black-box attacks on video recognition systems. In *Proceedings of the IEEE Symposium on Security and Privacy*, 2022.
- [52] Mintong Kang, Linyi Li, Maurice Weber, Yang Liu, Ce Zhang, and Bo Li. Certifying some distributional fairness with subpopulation decomposition. *Advances in Neural Information Processing Systems*, 35:31045–31058, 2022.
- [53] Chaowei Xiao, Ruizhi Deng, Bo Li, Taesung Lee, Benjamin Edwards, Jinfeng Yi, Dawn Song, Mingyan Liu, and Ian Molloy. Advit: Adversarial frames identifier based on temporal consistency in videos. In *Proceedings of the IEEE/CVF International Conference on Computer Vision (ICCV)*, pages 3968–3977, 2019.
- [54] Xiaojun Jia, Xingxing Wei, Xiaochun Cao, and Hassan Foroosh. Comdefend: An efficient image compression model to defend adversarial examples. In *Proceedings of the IEEE/CVF Conference on Computer Vision and Pattern Recognition*, pages 6084–6092, 2019.
- [55] Jeremy Cohen, Elan Rosenfeld, and Zico Kolter. Certified adversarial robustness via randomized smoothing. In *Proceedings of the 36th International Conference on Machine Learning*, pages 1310–1320. PMLR, 2019.
- [56] Jiang Liu, Chen Wei, Yuxiang Guo, Heng Yu, Alan Yuille, Soheil Feizi, Chun Pong Lau, and Rama Chellappa. Instruct2attack: Language-guided semantic adversarial attacks. *arXiv preprint arXiv:2311.15551*, 2023.

Appendix

1. Details for Experimental Setup

In style transfer stage, we use the following loss to iteratively update the input video:

$$L_{st} = \sum (\alpha L_{cont} + \beta L_{style} + \gamma L_{tv} + \delta L_{real}) + \lambda \sum L_{temp}, \quad (8)$$

where L_{cont} , L_{style} , L_{tv} , L_{real} and L_{temp} represents the content loss, style loss, total variance loss, realistic loss [36] and temporal loss respectively, α , β , γ , δ and λ are weight coefficients. In our experiments, we first fine-tune the parameters to achieve improved aesthetic results for visualization. We finally adopt the weight parameters as follows: $\alpha = 100$, $\beta = 10^6$, $\gamma = 10^{-4}$, $\delta = 5$, $\lambda = 20$. These parameter values were carefully chosen to strike a balance between style fidelity, content preservation, smoothness, and temporal consistency in the resulting video, but they can also be slightly changed if the attackers wish. We use PWC-Net [50] in optical flow estimation. We choose layer 4 of the pre-trained ResNet-50 model [33] as the output layer. In frame segmentation, SAM [13] provides three models (vit-h, vit-l and vit-b), which differ in backbone sizes. We use the default vit-h model to ensure the best segmentation accuracy.

2. Discussion

Other Video Attacks. Since LocalStyleFool is an unrestricted attack, it is unfair to compare it with a line of restricted attacks [7], [20]. We also do not compare our attack with universal attacks, which is another attack branch where the perturbations are first trained offline, and then applied to videos in the test/new data. Classic video universal

attacks include C-DUP (white-box) [8] and U3D (black-box) [51]. Universal attacks usually require high computational cost, since the attackers hope that adding trained universal perturbations to any video can cause misclassification. In most cases in this scenario, only untargeted attacks can be achieved. Therefore, due to different attack goals, it is also inappropriate to make comparisons between our attack and universal attacks.

Potential Mitigation. LocalStyleFool further unleashes the power of unrestricted attack by selecting local regions using SAM for perturbation superposition. In addition to the attack performance and naturalness of LocalStyleFool, its robustness against potential mitigations is also of interest to the attacker. Compared to attacks with ℓ_p -bounded perturbations, proactive defenses based on adversarial training [39], or more general distributional robust optimization [52], may offer little help in alleviating the local style-transfer-based attack. The reason is that it is a non-trivial task defining a proper adversarial risk to minimize, given the fact that the position and the style reference of the perturbations are unknown to the defender. On the other hand, considering that LocalStyleFool is superior to StyleFool in terms of consistency, consistency detection defenses (*e.g.*, AdvIT [53]) are even more unable to detect adversarial samples generated by LocalStyleFool. Image reconstruction defenses (*e.g.*, ComDefend [54]) may demonstrate certain defensive performance against the attack. These methods generally work based on the intuition that image reconstruction techniques have a chance to erase the adversarial perturbation or project it back to the manifold of the clean data distribution. Nevertheless, compared to global perturbations, local perturbations could be more resistant towards these defenses since the small perturbed regions have a higher chance of surviving from mitigation methods using random crops or random noise augmentation. Moreover, properly crafted locally stylized perturbations may better preserve the original distribution of the data, rendering image-reconstruction-based defenses less effective. Last but not least, LocalStyleFool also poses a threat against provable defenses, such as randomized smoothing [55]. The key challenge in applying randomized smoothing to defend against LocalStyleFool is that the perturbations, though only occupying some of the pixels in the inputs, can have a large ℓ_p magnitude which exceeds the certifiable radius of randomized smoothing. Since LocalStyleFool adds different style transfer to different regions, there might be insufficient smoothness in the splicing area between two adjacent regions. Therefore, a potential mitigation could be to detect the smoothness of color transitions. To conclude, it still requires efforts to propose effective defenses against LocalStyleFool and style-transfer-based attacks.

3. Future Prospect

In recent years, DNN-based models have been widely employed in various video-related tasks, including action recognition, video understanding, *etc.* Currently, the emergence of Large Language Models (LLMs) has prompted us

to pioneer an investigation into the deleterious effects of the Segment Anything Model when employed to attack DNN-based video recognition models. While conducting attacks on real-world commercial models proves to be financially burdensome due to the substantial computational resources required — approximately $10^3 \sim 10^4$ queries per video in digital attacks — we posit that the practical feasibility of such endeavors may be realized with the advent of query-efficient attack methodologies in the near future. Notably, the formidable capabilities of LLMs have been demonstrated in the image domain, wherein semantically meaningful adversarial perturbations have been generated by GPT-4 under the intentional guidance of the attacker [56]. Hence, an additional prospective avenue of research involves leveraging LLMs to actively generate adversarial videos, given their superior capacity for video comprehension compared to DNN-based models.